

# LOW MOMENTUM COMPACTION LATTICE OPERATION OF THE TAIWAN PHOTON SOURCE

C. C. Kuo, C. H. Chen, J. Y. Chen, P. C. Chiu, K. T. Hsu, K. H. Hu, C. H. Huang,  
 C. C. Liang, C. Y. Liao, Y. C. Liu, Z. K. Liu, H. J. Tsai, F. H. Tseng  
 National Synchrotron Radiation Research Center, Hsinchu 30076, Taiwan

## Abstract

In order to provide short bunch length for picosecond time-resolved experiments and for coherent IR/THz radiation, low momentum compaction factor ( $\alpha$ ) lattices have been commissioned recently at the Taiwan Photon Source (TPS). The momentum compaction can be positive or negative and its value can be reduced by more than two orders of magnitude. In this paper, we discuss variable low alpha lattice optics, its beam dynamics issues, the measured momentum compaction and bunch lengths as well as beam orbit stability issues, etc.

## INTRODUCTION

Coherent IR/THz radiation as well as incoherent short pulse radiation can be produced from picosecond electron bunches in a storage ring which could then be used for time-resolved experiments in the x-ray regime. With a low alpha lattice configuration, i.e, a quasi-isochronous lattice, the rms bunch length can be less than 1 picosecond at zero current in the TPS storage ring as reported in Ref. [1].

TPS is a 3-GeV, 3<sup>rd</sup>-generation synchrotron light source in Taiwan in which the first beam was stored by the end of 2014 [2] and a maximum stored beam current of 520 mA was reached during December 2015. Official public users operation began in September 2016 and currently routine users mode of operation is offered in 400 mA top-up mode.

The TPS lattice consists of 24 DBA cells, the natural emittance is 1.6 nm-rad for the nominal configuration and the 1<sup>st</sup> and 2<sup>nd</sup> order momentum compaction factors ( $\alpha_1$  and  $\alpha_2$ ) are  $2.4 \times 10^{-4}$  and  $2.1 \times 10^{-3}$ , respectively. With a 3.2 MV and 500 MHz radiofrequency system, the nominal zero-current bunch length is 10.8 ps rms and the bunch lengthening as a function of bunch current at different RF voltages were measured [3].

Recently, a number of low alpha lattices have been commissioned. As a result, a 3 nm-rad low emittance optics with  $\alpha_1 \sim 2.6 \times 10^{-5}$  could be established as a low alpha users mode for picosecond pulse experiments. A 40 nm-rad high emittance optics, on the other hand, can reach an  $|\alpha_1| < 1 \times 10^{-6}$ , and THz source characteristics as well as beam dynamics issues for the extremely short bunches can be investigated.

## LOW ALPHA OPTICS

We worked out a set of quadrupole settings with corresponding sextupole configurations to control lattice functions, betatron tunes, chromaticities,  $\alpha_1$ , and  $\alpha_2$ .

Two different optical types were investigated, and their natural emittances are around 3 nm-rad and 40 nm-rad, respectively. The low emittance optics can lower the first order alpha down to  $\alpha_1 \sim 2.6 \times 10^{-5}$ , but further reduction is constrained by sextupole hardware limits in the arc centers, in which strong fields are required to bring  $\alpha_2$  to near zero such as to preserve a sufficiently large longitudinal phase space for the stored beam. In the high emittance mode, some sextupoles need polarity switching, done initially manual and later electronically after installation of remote switching devices [4]. Figure 1 shows the optical functions and Table 1 lists the major parameters and the zero-current bunch lengths at 3.2 MV RF voltage.

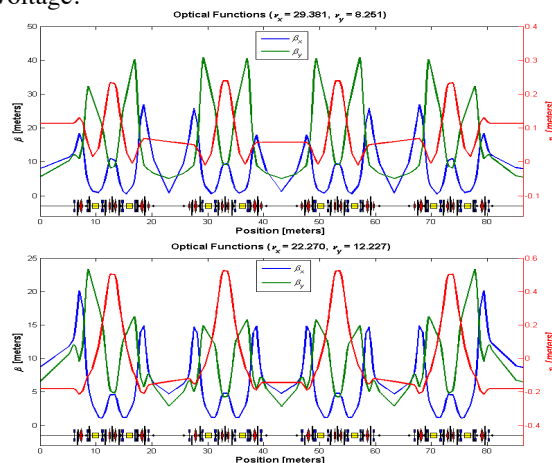


Figure 1: Low alpha, low emittance ( $\alpha_1=2.6 \times 10^{-5}$ ,  $\epsilon=2.9$  nm-rad) lattice functions (above); and low alpha, high emittance ( $\alpha_1=-2.94 \times 10^{-6}$ ,  $\epsilon=40.1$  nm-rad) lattice (below).

Table 1: Major Parameters of the Low Alpha Lattices

Parameter	Low emittance	High emittance
Emittance (nm-rad)	2.9	40.1
$\alpha_1$	$2.60 \times 10^{-5}$	$-2.94 \times 10^{-6}$
$\alpha_2$	$7.15 \times 10^{-4}$	$-3.51 \times 10^{-5}$
$\alpha_3$	$-2.28 \times 10^{-3}$	$-2.75 \times 10^{-2}$
Tune $\nu_x/\nu_y$	29.381/8.251	21.270/12.227
$\sigma_1$ (ps), RF=3.2 MV	3.3	1.1
Nat. Chrom. $\xi_x/\xi_y$	-65/-46	-36 /-23

## ALPHA AND BUNCH LENGTH MEASUREMENT

### Low Emittance, Low Alpha Lattice

Rather than reversing polarity of one quadrupole family as described in the previous design report [1], we turned them off because of their low strengths. As stated in [1],

Content from this work may be used under the terms of the CC BY 3.0 licence (© 2018). Any distribution of this work must maintain attribution to the author(s), title of the work, publisher, and DOI.

we can only reach  $\alpha_1 \sim 2.6 \times 10^{-5}$  due to strength limitation in sextupoles. The beam injection efficiency was  $\sim 50\%$  and the lifetime was around 6 hrs at 30 mA. The optical functions were corrected by LOCO [5]. Varying the measured synchrotron tune by changing the RF frequency, we can get  $\alpha_1$  and  $\alpha_2$  (neglecting higher order terms) according to equation [6]:

$$v_s = \sqrt{\frac{heV_{rf} \cos \phi_s}{2\pi E}} (\alpha_1^2 - 4\alpha_2 \frac{\Delta f_{rf}}{f_{rf}})^{1/4}.$$

Another method to derive the alphas is to measure the closed orbit change while varying RF frequency (energy). But due to large dispersion-like orbit distortions around 0.3 Hz and 3 Hz (ocean waves and crust resonances), especially for the high emittance cases at very low  $\alpha_1$ , we got large uncertainties in  $\alpha_2$ . The measured alphas and the model values are listed in Table 2.

A dual-sweep streak camera (C10910 Hamamatsu Photonics) with picosecond resolution is employed to measure the bunch length [7]. Figure 2 shows the measured bunch length as a function of bunch current for the nominal users mode together with other low alpha cases (low emittance lattices). It demonstrates, there is a possible users mode with 6.5 ps rms at a bunch current of 0.1 mA and 3.2 MV RF voltage for  $\alpha_1 \sim 2.6 \times 10^{-5}$ . The total beam current could be as high as 60 mA when 600 bunches are filled in the ring.

Table 2: Model and Measured Alphas

	Model	$v_s$ vs $\Delta f_{rf}$	COD vs $\Delta f_{rf}$
$\alpha_1$	$2.60 \times 10^{-5}$	$2.84 \times 10^{-5}$	$3.0 \times 10^{-5}$
$\alpha_2$	$7.15 \times 10^{-4}$	$6.25 \times 10^{-4}$	$1.2 \times 10^{-3}$

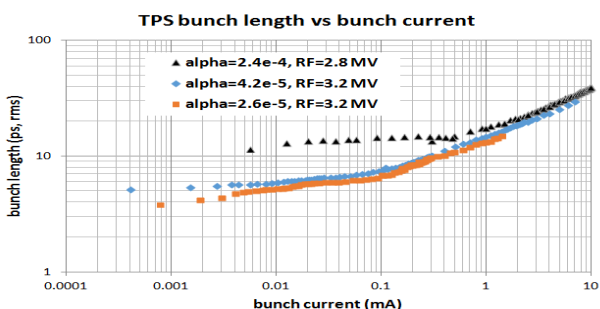


Figure 2: Measured bunch length vs bunch current in low alpha and normal users modes of operation.

### High Emittance, Low Alpha Lattice

We began beam tests with the  $\alpha_1 \sim 1 \times 10^{-6}$  lattice and found it was very difficult to accumulate a stored beam without further calibration of the lattice functions, RF frequency adjustment and orbit noise suppression. Therefore, we started with the  $\alpha_1 \sim 2 \times 10^{-5}$  lattice instead. Following a LOCO procedure, the lattice functions were corrected. We then changed the focusing quadrupoles in the arc centers to lower  $\alpha_1$ . With proper chromaticity settings and  $\alpha_2$  in the beginning, we kept sextupoles values while varying  $\alpha_1$ . Betatron tunes were optimized

using quadrupoles near the straight sections. RF frequency was carefully adjusted to compensate for any ring path length change, especially for the extremely low  $\alpha_1$  case in which a significant energy offset can easily be introduced. During every machine study, we needed to restore the previous RF frequency setting and fine tuning was necessary. Moreover, RF phases in two RF systems needed to be matched to provide the proper longitudinal phase space for the injected beam. Figure 3 shows the measured  $\alpha_1$  for various quadrupole focusing settings. We reached about 30% injection efficiency for  $\alpha_1 = 6 \times 10^{-6}$  and, by slightly shifting focusing quadrupoles, even an  $\alpha_1 = 3 \times 10^{-7}$  could be achieved. The measured bunch length using a streak camera for the very low alpha configuration is shown in Fig. 4. The case in Fig. 2 with 3.2 MV RF voltage is scaled to 2.8 MV.

Bunch lengthening effects for different positive alphas using Haissinski's solution for an R+L impedance of the TPS storage ring ( $R=2005\Omega$ ,  $L=51nH$  in Ref. [3]) are plotted in Fig. 4. Comparing with the measured bunch lengths, the discrepancies might be due to streak camera resolution, errors due to aberration in a focusing mirror (about 1 ps reduction using a bandpass filter), etc. Moreover, we should be aware of the intrinsic limit of bunch length due to longitudinal quantum radiation excitation and transverse longitudinal coupling at extremely low alpha [8-9]. The negative alpha cases show a microwave instability threshold current which is higher.

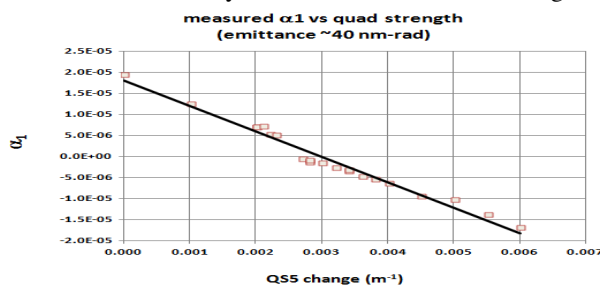


Figure 3: Measured  $\alpha_1$  vs central quadrupole strength for the high emittance lattice.

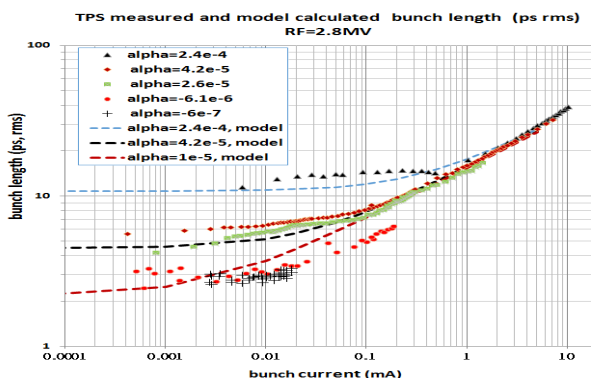


Figure 4: Measured bunch lengths using a streak camera as a function of bunch current for very low positive and negative alpha, and in normal users mode. Calculated model bunch lengths are plotted.

## ORBIT STABILITY

Transverse beam motion for the low alpha lattice has been measured and it shows that, in the horizontal plane, the closed orbit has a dispersion-like pattern which is much larger than in the nominal lattice. Theoretically, the closed orbit is generated by error sources like:

$$x_i = \sum_j \left( \frac{\sqrt{\beta_i \beta_j}}{2 \sin \pi \nu} \theta_j \cos(|\phi_i - \phi_j| - \pi \nu) + \delta \eta_i \right)$$

$$\delta = -\frac{1}{\alpha} \left( \frac{\Delta C}{C} - \frac{\Delta f_{RF}}{f_{RF}} \right) \Delta C = \sum_j \theta_j \eta_j \approx \sum_j K_j L_j \eta_j \langle \Delta x_{quad} \rangle$$

The dispersion-like orbit could be from RF frequency noise, kicks in the dispersion region, e.g., orbit offsets in the quadrupoles in dispersion region, etc.

Measured horizontal orbit power densities for three different alpha cases without orbit feedback are shown in Fig. 5. The bumps around 0.3 Hz and 3 Hz are from ocean waves and crust resonances in the island of Taiwan, respectively. The 29-Hz peak in the  $\alpha_1 = -6 \times 10^{-6}$  case is due to one of the dry pumps in operation. Higher frequency peaks at 60 Hz harmonics come from noise in an analog part of the RF low level control electronics which could be reduced after its replacement with a digital type.

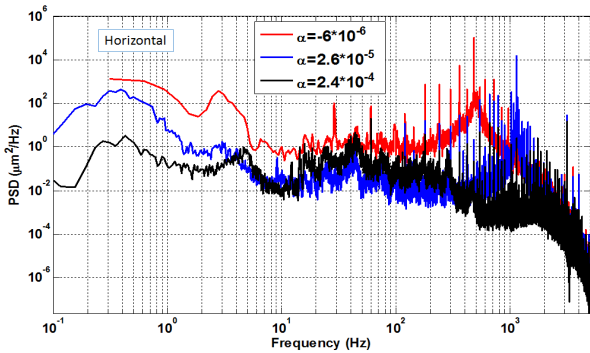


Figure 5: Measured horizontal orbit power densities for three different alpha cases without orbit feedback. Note that one of the dry pumps in operation induces 29-Hz peak in the  $\alpha_1 = -6.0 \times 10^{-6}$  spectrum. The other two cases are with all dry pumps off. Dispersion functions at measured location for  $\alpha_1 = 2.4 \times 10^{-4}$ ,  $2.6 \times 10^{-5}$ , and  $-6.0 \times 10^{-6}$  are 0.23, 0.24 and 0.51 m in black, blue and red lines, respectively.

A fast orbit feedback system (FOFB) combined with an RF frequency compensation loop was used to suppress the orbit noise within sub-micron level for the routine operation lattice ( $\alpha_1 \sim 2.4 \times 10^{-4}$ ) [10]. This FOFB was also applied to the low alpha mode. For the emittance 3 nm-rad,  $\alpha_1 \sim 2.6 \times 10^{-5}$  lattice, we activated the FOFB and the orbit could be maintained within sub-micron tolerance up to 100 Hz horizontal and 300 Hz vertical, respectively. The measured horizontal orbit power densities and integrated orbit as a function of frequency are shown in

Fig. 6. The orbit trend sampled at a 1 Hz rate for this low alpha mode with FOFB on and off while varying one ID gap is plotted in Fig. 7.

## DISCUSSION

Two different low alpha lattice modes have been commissioned at the TPS storage ring. The momentum compaction factor could be reduced by more than two orders of magnitude and the measured bunch lengths were within a few ps as observed with a streak camera. A low emittance mode of 3 nm-rad could be adopted as a user operation mode to provide short, ps radiation pulse capability. The orbit stability was kept at sub-micron level using a fast orbit feedback system. Further studies are needed for beam dynamics issues at extremely low alpha conditions and for a measurement of the coherent IR/THz spectrum.

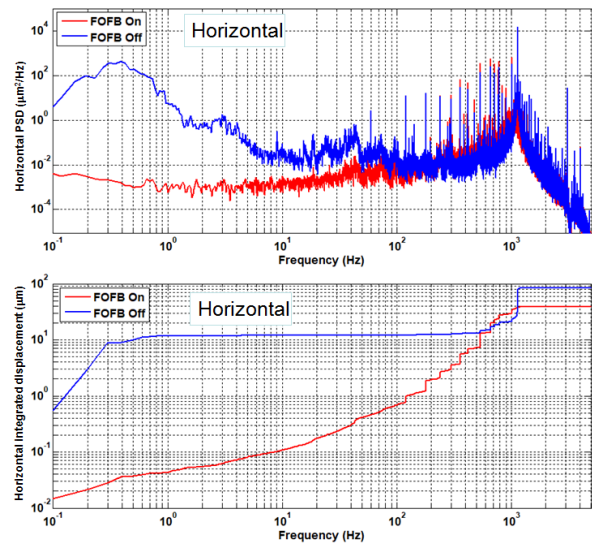


Figure 6: Measured horizontal orbit power densities (above) and integrated orbit displacements (below) at high dispersion location with and without orbit feedback in the low emittance lattice with  $\alpha_1 \sim 2.6 \times 10^{-5}$ .

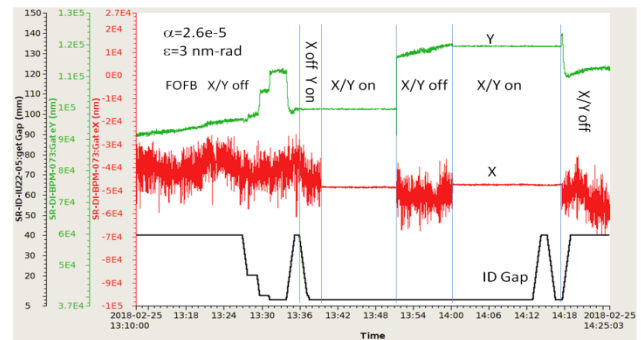


Figure 7: Orbit trend sampled at a 1 Hz rate for the  $\alpha_1 \sim 2.6 \times 10^{-5}$  lattice with FOFB on and off while varying one ID gap.

## ACKNOWLEDGEMENT

We thank A.W. Chao and X. Huang of SLAC for advice on this work.

## REFERENCES

- [1] C. C. Kuo and H.J. Tsai, "Design of low momentum compaction lattices for the TPS storage ring", in *Proc. IPAC '13*, Shanghai, China, May 2013, paper MOPEA060, p. 217.
- [2] C. C. Kuo *et al.*, "Commissioning of the Taiwan Photon Source", in *Proc. IPAC '15*, Richmond, VA, USA, May 2015, paper TUXC3, p. 1314.
- [3] C. C. Kuo *et al.*, "Impedance study with single bunch beam at Taiwan Photon Source", in *Proc. IPAC '16*, Busan Korea, May 2016, paper MOPOR016, p. 630.
- [4] Y. S. Wong *et al.*, "Modification of a power supply for low-alpha operation in the Taiwan Photon Source", presented at IPAC'18, Vancouver, Canada, May 2018, paper THPAL054.
- [5] F. H. Tseng *et al.*, "Optics calibration and measurement for low alpha lattices in TPS storage ring", presented at IPAC'18, Vancouver, Canada, May 2018, paper THPAK054.
- [6] A. Nadji *et al.*, "Quasi-isochronous experiments with the Super-ACO storage ring", *Nucl. Instr. Meth.*, vol. 378, p. 376, 1996.
- [7] C. Y. Liao *et al.*, "Synchrotron radiation measurement at Taiwan Photon Source", in *Proc. IBIC'15*, Melbourne, Australia, Sept. 2015, paper TUPB067, p. 507.
- [8] Y. Shoji, *et al.*, "Longitudinal radiation excitation in a storage ring", *Phy. Rev. E.*, vol. 54, no. 5, R4556, 1996.
- [9] Y. Shoji, "Bunch lengthening by a betatron motion in quasi-isochronous storage rings", *Phy. Rev. ST, Accel. Beams*, vol. 7, p. 090703, 2004.
- [10] P. C. Chiu, *et al.*, "Orbit correction with path length compensation based on RF frequency adjustments in TPS", in *Proc. IPAC '17*, Copenhagen, Denmark, May 2017, paper TUPAB103, p. 1553.